

Bio-inspired Backlash Reduction of a Low-Cost Robotic Joint Using Closed-loop Commutated Stepper Motors

József Veres · György Cserey · Gábor Szederkényi

2012

Abstract The majority of current robotic joints are primarily actuated by rotational mechanisms. These electrical drives have substantially different features than the features found in human muscular systems. This paper presents a cost-effective solution to the backlash a phenomenon known to cause positioning errors and other **undesirable** dynamic effects in drives. These errors are particularly pronounced when relatively **major** changes appear in the preload conditions of the motor such as in the case of a robotic leg or arm with a high degree of freedom. Current solutions require an accurate time-varying model of the drives that is not available in the majority of practical cases. Therefore, a digitally-controlled mechanical solution is proposed in this paper that is inspired by the human flexor-extensor mechanism. The idea is to construct an antagonistic actuator pair that is analogous to the flexor and extensor muscles. In order to obtain good control performance even in the low speed range, permanent magnet stepper motors were chosen as actuators that are commutated in a digital closed-loop fashion. The operation of the controlled structure has been verified in a real experimental environment where measurements showed good results and **good match** with previous simulations.

Keywords backlash · robotic joint · permanent magnet stepper motor · closed-loop commutation ·

József Veres
Práter utca 50/a, Budapest H-1083, Hungary
E-mail: veres.jozsef@itk.ppke.hu

György Cserey
Práter utca 50/a, Budapest H-1083, Hungary
E-mail: cserey.gyorgy@itk.ppke.hu

Gábor Szederkényi
P.O. Box 63, Budapest, H-1518, Hungary
E-mail: szeder@sztaki.hu

electric drives · transmission · mechatronics · drives · motion control

Nomenclature

b	Measure of a backlash as a distance [m]
β	Measure of a backlash as an angle [rad]
r	Radius of a gear [m]
τ	Torque [Nm]
i	Current [A]
I	Nominal current [A]
θ	Angle [rad]
J	Inertia [kgm ²]
B	Viscous friction [Nms/rad]
F	Force [N]
ω	Angular velocity [rad/s]
n	Gear ratio
N	Pole number
x	Linear position [m]
k	Feedback strength [1/s]
K	Stiffness [N/m]
e	Angle difference [rad]
E	Angle difference threshold [rad]
T	Time period [s]

Subscripts

m	Motor
a, b	Phase a and b
p	Pole
g	Intermediate gear
l	Load (real)
L	Load (estimated)
r	Reaction
d	Desired
c	Computed
t	Total
j	Index of the elements in pair (1,2)

1 Introduction

Most robotic joints are actuated by rotational mechanisms. Typically, these mechanisms are driven by electric motors whose operating speed is higher than what the joints actually require. Gearboxes are then used to reduce the speed of the joints and also to increase their torque. The incorporation of a gearbox corrupts the continuity of the torque transmission in most cases because of the backlash phenomenon. Backlash originates from the gear play that results from the imperfectness of the fabrication or the increased wear level of the mating gears. During static motion this introduces only positioning errors but in dynamic cases limit-cycles may occur. Some mechanical and control solutions that reduce the effect of backlash are given below.

Starting with the control solutions it can be concluded that numerous publications are available in the field. Most of these papers offer solutions for the modeling and identification of the mechanical system together with the backlash phenomenon [1–6]. Different approaches include vibration analysis [7], wavelet analysis [8], utilizing fuzzy logic [9] and Kalman filters [10]. Compensation of the effect of the backlash using Stribeck friction was reported in [11] and [12]. Controllers and adaptive controllers for mechanical systems with backlash can be found in [13–15]. There are papers focusing on different applications like positioning [16] or target tracking [17]. Hovland *et al.* [18] showed a backlash identification in robot transmission. Backlash compensation for a humanoid robot with a disturbance observer [19], as well as with a genetic algorithm [20], were reported. Turning now to mechanical solutions, a few examples include anti-backlash gears, pre-loaded gears, and harmonic drives. The latter were originally developed for aerospace and military applications and offer a very low level of backlash with high reduction ratios in a compact size. These advantages have made the harmonic drive the most widely used robotic gear type. The disadvantages of using this type of mechanical solution are its increased level of elasticity and its significantly higher cost.

The cost of the actuator can be an issue, for example in the cases where high degree of freedom (DOF) robots are needed. Good examples of this are the humanoid or biped robots where tens of joints are usually required to be actuated. In almost all cases these are series manipulators. According to Akhter *et al.* [21] a large percent of these robots are not equipped with harmonic drives but use standard gears presumably to be more cost effective but at the same time suffering from the effect of backlash.

In this work, a low-cost alternative solution for decreasing the effect of backlash in robotic joints is presented. This solution reduces backlash by incorporating a flexor-extensor pair of low-cost PM stepper motors bundled with low-end integrated gearboxes. The method was inspired by the biological structure of human limbs, which inspiration is briefly introduced in the following section.

There are related studies in the literature. For parallel manipulators Sven *et al.* [22] and Boudreau *et al.* [23] have recently published their dual motor mechanism that can be used to reduce the level of backlash. The original level was reported to be reduced by over 90%. Turning to the series manipulators, which is only in the scope of this paper, Kiyoshi *et al.* [24, 25] presented their twin-drive mechanism that is related to the solution of this paper. They were using direct-drive DC motors, which creates a significant limitation since without gears the robots that are in the scope of this paper could not be built due to the lack of the adequate torque capability.

It has to be emphasized that this paper does not target the area of the classical industrial manipulators — where precision and repeatability are more important than the cost of the actuators — but the robots with high DOF that require negligible backlash at low-cost.

The paper is divided into seven sections. In the next section, the inspiring mechanism is presented. The description of the proposed robotic joint is in the third section. The fourth section contains the nonlinear model of the joint. The algorithm of the motion control appears in the fifth section. The sixth section contains the results of the simulations and experiments, and in the last section, the contributions of the work are summarized.

2 The Inspiring Human Flexor-Extensor Mechanism

Human muscles can only exert force in one direction. This is why it is always necessary to have counterparts to be able to create repetitive motion with the help of cyclic contractions, like walking. These muscle groups are called the agonists and the antagonists. Well known examples are the biceps brachii and triceps brachii muscles of the upper arm. By using these antagonistic pairs we are able to perform a wide variety of motions. For example, if the two antagonistic muscles are contracted simultaneously, it is possible to change the stiffness of the joint. In terms of precise co-ordination of these muscle groups, complex neural controls are generally required. However, simple reflex-arcs exist that can realize fast but very simple reactions [26]. A good example of this is the collateral inhibition of the antagonist-

tic muscles that serves as a basic mechanism of muscle co-operation. This idea inspired the authors to design and implement an alternative solution for the backlash problem of low-cost robotic joints.

Our approach is to use a pair of low-cost actuators instead of a more expensive solution that contains a harmonic drive. Then one actuator is dedicated for the right turn and the other for the left turn like the flexing and extending in the human limbs. A smooth motion can be realized with a proper control by mimicking a simple reciprocal innervation of the two muscle groups. The main advantage of this approach is that the backlash of the joint can be almost completely eliminated with a simple digital control that is implemented using a low-end microcontroller.

3 Description of the proposed robotic joint

As it was introduced in the previous sections this approach uses a pair of actuators. These include gearboxes with a significant level of backlash. Fig. 1 shows the structure of the proposed joint. The two actuators that are facing in an opposite direction are attached to a fixed body (Link 1). The outputs of the gearbox axes are directly coupled with the output of the robotic joint that is actuated (Link 2). The following convention is used: Motor 1 is assigned to the right turn (flexing) and Motor 2 for the left turn (extending). This could be arbitrarily set but the above written convention is used. The gearboxes are low-end spur type and are integrated with the PM stepper motors. These are three stage gearboxes with a gear reduction ratio of 100:1 ($n_1 = n_2 = 10$). The total backlash (β_i) of the individual gearboxes is 0.0192 *rad*. Nowadays the permanent magnet stepper motors are becoming affordable and widely used not only in the industry but even in the field of aerospace engineering [27]. These motors or the hybrid types combined with a simple microcontroller can perform well [28–31] even in the low speed region.

In order to actuate the joint, low-cost, two-phase, bipolar permanent magnet stepper motors were chosen. Each of these has six pole-pairs with 8 Ω coil resistance and 24 *mH* coil inductance. The nominal currents are 0.45 *A* with holding torques of 0.012 *N·m*. The inertia of the rotors are $1.5 \times 10^{-6} \text{kg} \cdot \text{m}^2$ with motor constants of 0.004 *N·m/A*. Both motors are equipped with on-axis rotary encoders. Non-contacting sensor is the type that is the most widely used nowadays since these are less prone to wear out. Optical encoders are used as standards but recently the magnetic type rotary encoders are getting to become a good alternative solution. The

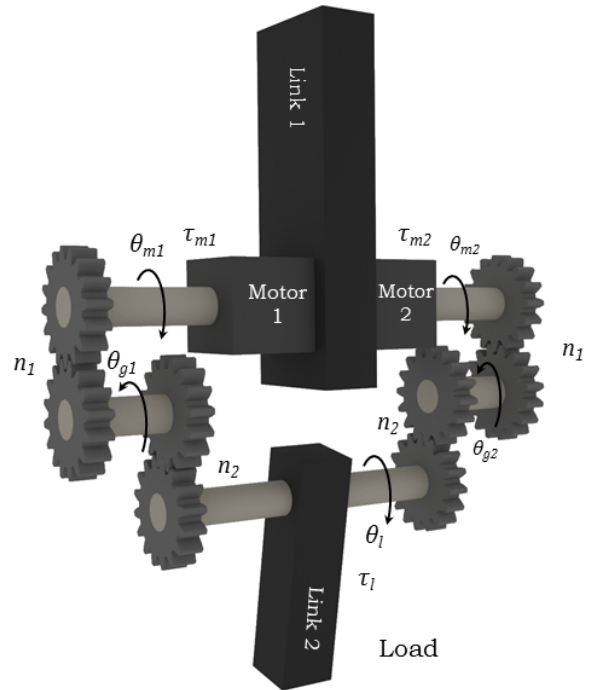


Fig. 1 Electromechanical model.

latter one offers a cost effective way of angular measurement at the price of the decreased maximal spatial resolution. In this paper AS5045 type sensors are used that provide 12 bit absolute resolution. This is equivalent to a 4096 CPR that is acceptable for these robots. The sampling rate of the sensor is 10.4 *KHz*. Besides the two sensors that measure the angular position of the two motors, one more sensor is used. It is optional, but the reason why it is used here is to assist the verification of the backlash reduction.

The implemented prototype is shown in Fig. 2. The two PM stepper motors are denoted by (A) and the corresponding gearboxes by (B). On the top of the motors (C) denotes the magnetic encoders and the driving circuits. A3979 is used as a motor driver along with a PIC24HJ12GP202 16bit microcontroller. The driver features internal PWM current control which reference value is updated by the microcontroller. (D) marks the optional load side encoder that measures the angular position of Link 2 respective to Link 1. The letters (E) and (F) indicate Link 1 and Link 2 respectively. The full motion control algorithm is implemented onboard that means a PIC24FJ16GA002 microcontroller responsible for the complete digital control (G). Personal computer is used only for data acquisition.

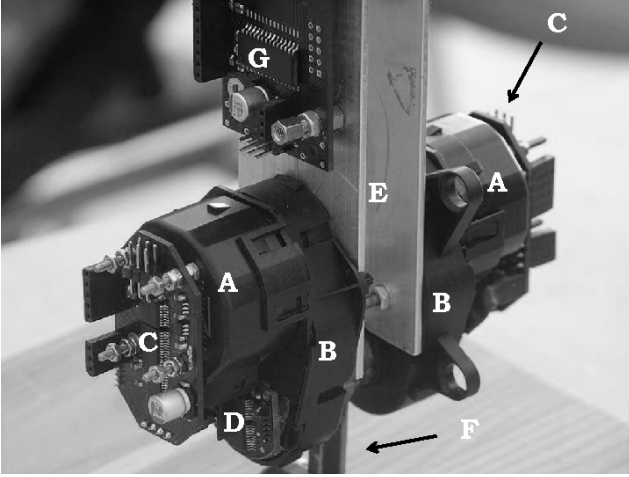


Fig. 2 Photo of the implemented prototype.

4 Modeling of the joint

4.1 Stepper motor model

The instantaneous torque of the permanent magnet stepper motor can be written as: [32]

$$\tau = -K_m [i_a \sin(N_p \theta) - i_b \cos(N_p \theta)], \quad (1)$$

where K_m ($N \cdot m/A$) is the motor constant, i_a (A) is the current in phase a , i_b (A) is the current in phase b , N_p is the number of the rotor poles, and θ (rad) is the mechanical angle of the rotor.

Fig. 3 shows this static torque characteristic. It is modeled as a sinusoid-like function of the rotor's angular position where the higher harmonics like the 4th harmonic (the cogging torque) are neglected. Both the one-phase and the two-phase excitations are plotted (the latter two-phase excitation was chosen since it offers more torque). The static torque is normalized and the stable points (o), that represent the rotor's rest position if no external load applied, are marked.

Then the differential equation of the motor's dynamic is given by [33]:

$$\frac{d^2\theta}{dt^2} = \frac{-K_m i_a \sin(N_p \theta) + K_m i_b \cos(N_p \theta) - B\omega}{J} \quad (2)$$

where ω (rad/s) is the mechanical angular velocity, B ($N \cdot m \cdot s/rad$) is the viscous friction coefficient and J ($Kg \cdot m^2$) is the inertia of the rotor.

The coils are excited with full-stepping method that can be written up in the following way [34]:

$$i_a = I \sin(N_p \theta_d) \quad (3)$$

$$i_b = I \cos(N_p \theta_d), \quad (4)$$

where I (A) is the nominal current of the motors' coil and θ_d is the desired angle where $\theta_d \in [\frac{\pi}{4}, \frac{3\pi}{4}, \frac{5\pi}{4}, \frac{7\pi}{4}]$.

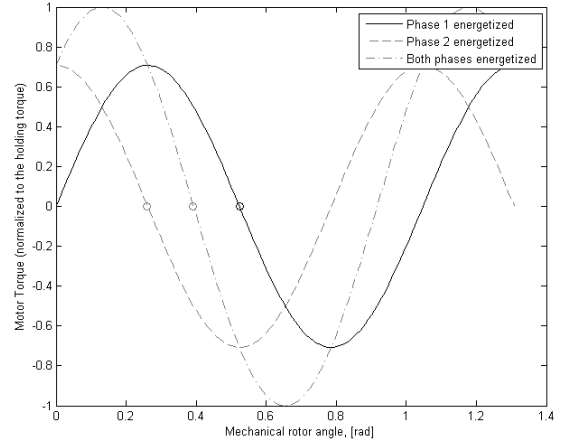


Fig. 3 Normalized static torque characteristic of the stepper motor.

4.2 Gear train and backlash model

First assume that the transmission of the motors are free of backlash and all the elastic deformations are neglected. In this case the angular position of the load can be written in the following forms:

$$\theta_l = \frac{\theta_{m1}}{n_1 n_2} = \frac{\theta_{g1}}{n_2} = \frac{\theta_{m2}}{n_1 n_2} = \frac{\theta_{g2}}{n_2}, \quad (5)$$

where n_1 is the reduction ratio between the first and the second stage and n_2 is between the second and the last stage. This linear formula turns to be highly non-linear once the effect of the backlash is added. Two different scenarios are usually distinguished. Contact Mode (CM) when the two mating gears are in contact and the Backlash Mode (BM) when these are disengaged [13]. Fig. 4 shows a gearplay between mating

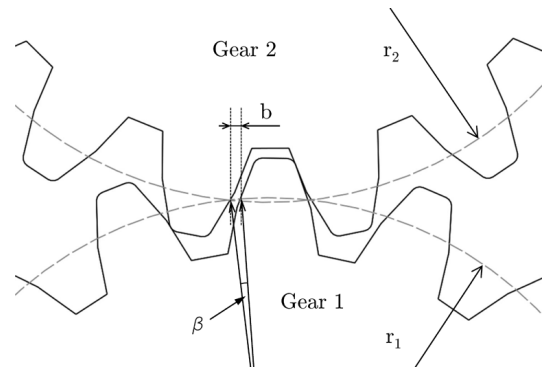


Fig. 4 Illustration of the backlash

gears. The value of the backlash measured as a linear distance is denoted by b . It can be approximated by

using the angle β (rad) and the radius r_1 as:

$$b \approx \beta r_1, \quad (6)$$

since β is a small angle. Similarly it is equal to the radius of Gear 2 multiplied by the angle of backlash measured on the second gear. In the literature there are different approaches to model the effect of the backlash [4, 5, 10, 15]. One of these is the contact model type that is using non-linear reaction forces [14]. The idea is to model the occurring contact between the mating gears with a non-linear elastic force that depends on the relative position (x) of the mating gears. The starting point ($x = 0$) is when the gears are at the center of the empty space. The relative position of the mating gears is defined as:

$$x = r_1\theta_1 - r_2\theta_2, \quad (7)$$

For simplicity, a piecewise linear function is used to express the reaction forces, that can be seen in Fig. 5.

$$f(x) = \begin{cases} K(x + b/2) & x < -b/2 \\ 0 & |x| \leq b/2 \\ K(x - b/2) & x > b/2 \end{cases} \quad (8)$$

The stiffness K and individual backlash b values are expected to be identical for all the stages of the gear trains. The numerical values are approximated by experimental results that are presented in the sixth section. By using (7) the reaction force acting on the teeth of Gear 1 can be defined as:

$$F_r = f(r_1\theta_1 - r_2\theta_2), \quad (9)$$

and the torques of gear 1 and 2, created by the reaction forces acting on the mating teeth are given by:

$$\tau_1 = F_r r_1 \quad (10)$$

$$\tau_2 = -F_r r_2. \quad (11)$$

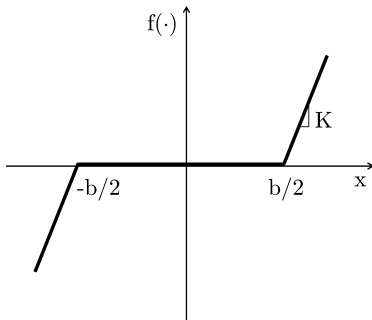


Fig. 5 Piecewise linear function for backlash modelling.

4.3 Complete model

The complete electromechanical model of the proposed joint is modeled as a five-inertia system that includes backlash and viscous friction. According to the naming conventions of Fig. 1, the index of m refers to the motor number and the first stage of the gearbox, g to the second stage, and l to the load and the last stage. Then by using (2), (6) and (9) the complete model becomes:

$$\frac{d^2\theta_{m_j}}{dt^2} = \frac{\tau_{m_j} - B_m\omega_{m_j} - F_{mg_j}r_m}{J_m} \quad (12)$$

$$\frac{d^2\theta_{g_j}}{dt^2} = \frac{-B_g\omega_{g_j} + F_{mg_j}r_{gm} - F_{gl_j}r_{gl}}{J_g} \quad (13)$$

$$\frac{d^2\theta_l}{dt^2} = \frac{\tau_l - B_l\omega_l + (F_{gl_1} + F_{gl_2})r_l}{J_l} \quad (14)$$

$$\tau_{m_j} = -K_m [i_{a_j} \sin(N_p\theta_{m_j}) - i_{b_j} \cos(N_p\theta_{m_j})] \quad (15)$$

$$i_{a_j} = I \sin(N_p\theta_{d_j}) \quad (16)$$

$$i_{b_j} = I \cos(N_p\theta_{d_j}) \quad (17)$$

$$F_{mg_j} = f(\theta_{m_j}r_m - \theta_{g_j}r_g) \quad (18)$$

$$F_{gl_j} = f(\theta_{g_j}r_g - \theta_l r_l), \quad (19)$$

where j , that can be 1 or 2, denotes the element of the actuator pair. The B coefficients are the viscous damping coefficients and τ_l represents all the external forces acting on the load. J_m denotes the combined inertia of the motors and the first stage. J_g is the inertia of the intermediate stage and J_l indicates the inertia of the load and the last stages. The numerical values were numerically computed on the available CAD drawings of the parts. The forces F_{mg_j} are the reaction forces acting on the mating gears of the first stage (m) and the intermediate stage (g), and similarly F_{gl_j} is the reaction force of the intermediate and the last stage (l).

5 Motion control

The control input to the system is the angular velocity reference (ω_{ref}) of the joint. As a first assumption this specifies the rate of change of the desired positions of the two motors. This means that the desired angular velocities of the motors are given by:

$$\omega_{d_1} = \omega_{ref} \quad (20)$$

$$\omega_{d_2} = -\omega_{ref}. \quad (21)$$

An open-loop commutation scheme could enforce the desired angular velocity command if proper acceleration and deceleration phases were added in order to prevent the loss of synchronism. That would imply the commonly used trapezoidal speed profile. Unfortunately even that could not guarantee the synchronism in the

presence of unknown external loads, therefore closed-loop commutation is used. In order to keep the commutation synchronised with the rotor, error variables are defined for feedback that are defined as:

$$e_j = \theta_{m_j} - \theta_{d_j} \quad (22)$$

Fig. 6 shows the flowchart of the two individual motor commutation. In order to prevent the loss of synchronism, if the error is greater than a predetermined threshold ($E=0.2 \text{ rad}$), the current step is delayed until it falls below the threshold.

The closed-loop commutations of the stepper motors are just the low-level parts of the whole motion control. The high level part is responsible for the generation of the commanded angular velocities (ω_{cmd_j}). The block diagram of the complete motion control can be seen in Fig. 7. In order to reduce the level of backlash a cross-connected feedback is taken. β_d is the desired level of angle difference and it is defined as:

$$\beta_d = b_t r_m = \beta_t n_1 n_2, \quad (23)$$

where b_t is the total backlash of the gearbox given as a linear distance, β_t is the angle of the total backlash expressed at the last stage and k is a constant that sets the strength of the error feedback. As it can be seen in Fig. 7 the control tries to drive the actuators on the two sides (flexor and extensor) in a way to make $\beta_d - (\theta_{m_1} - \theta_{m_2})$ approach zero. The closer it drives to zero the less the resulting backlash is. Then the position of the load can be approximated by:

$$\theta_l \approx \frac{\theta_{m_1} + \theta_{m_2}}{2n_1 n_2} = \theta_L. \quad (24)$$

Since θ_l is also measured, the comparison of the two trajectories become a good benchmark for the operation of the system.

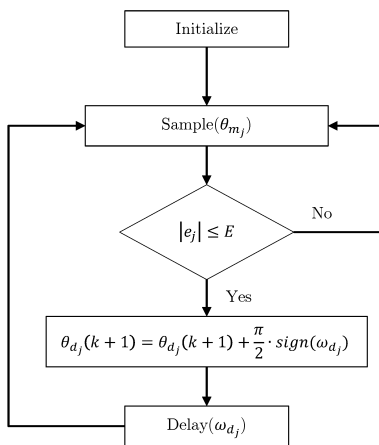


Fig. 6 Flowchart of the closed-loop commutation.

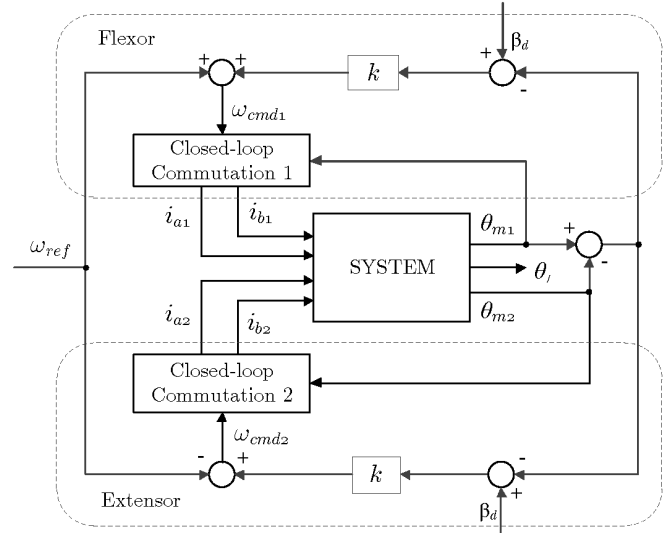


Fig. 7 Block diagram of the motion control of the joint.

6 Simulation and experimental results

For running the simulations MATLAB 8 was used with the help of the built-in numerical differential equation solver that is based on the variable step Runge-Kutta method.

In order to create a basis for comparison a new system is introduced. If one of the flexing-extending actuator pair is removed, a standard robotic joint would be achieved. Let the actuator denoted by index $j = 2$ be omitted, which means the motor and the gears are physically removed. The corresponding complete model is the same as was derived previously but j is limited to one and F_{gl_2} is set to be zero. In the following, it is referred to as the *standard case* and the original one as the *flexor-extensor case*.

Fig. 8(a) and Fig. 8(b) illustrate two of the model validation results where the standard case was used. Both figures show the measured and simulated θ_l load positions as two different τ_l external load torques were applied at about $t = 0.6s$. The motors were excited with the maximum constant current in order to produce the maximum holding torque, that prevented the applied external torque to backdrive the motor. The position of the load was set to one extremum of the empty space created by the gearplay.

Then the applied external torque forced the load to move towards the other extremum. The smaller $0.5Nm$ torque created a small overshoot that corresponds to the impact of the mating gears. The load position after the impact is just slightly bigger than the original backlash of the gearbox. The larger one caused a bigger impact and showed a damped oscillatory motion with a

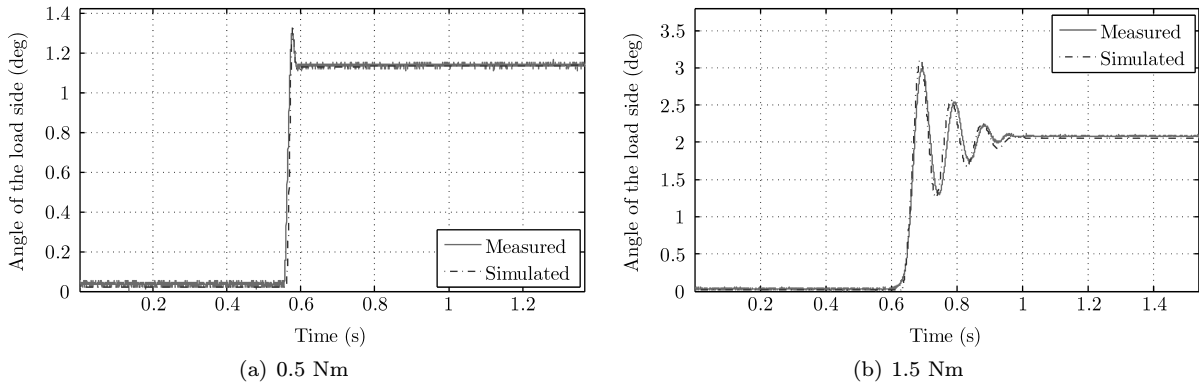


Fig. 8 Results of the model validation.

settled position equal to almost the twice of the original backlash.

Fig. 9 and Fig. 10 show the comparison of the new flexor-extensor approach with the standard approach. In both cases the angular velocity reference (ω_{ref}) was given. In order to realize a smooth back and forth motion, that is needed to analyze the moment of the direction change, sinusoidal velocity reference was given.

Fig. 9(a) shows the simulation results of the directly measured (θ_I) and approximated (θ_L) position of the load. Since there is no external disturbance the position of the load follows the position of the motors with a small difference. The difference between the two curves is enlarged in Fig. 9(c).

As the motion of the motors change direction the mating gears smoothly travel the empty space caused by the backlash. First, it creates positional inaccuracy and furthermore in the presence of external disturbances (e.g.: caused by other joints) it can create high impacts that has been shown in Fig. 8(b). The real measurement is showed in Fig 9(b) and the zoomed counterpart is also depicted in Fig. 9(c). The measured curves show the raw signals that are not filtered and therefore contain some noise.

Now turning to the new approach proposed in the paper the simulation results obtained by using the flexor-extensor case depicted in Fig. 10(a). By using the identical reference velocity that was used before and recording the same system variables, the difference between the two curves disappear. The enlargement in Fig. 10(b) also shows a significant reduction. The experimental results of this approach shows similar effect in Fig. 10(c). By zooming into the curves in Fig. 10(d) small deviations, that are comperable to the noise base of the sensor, become only noticeable.

However, precise measurement of the position dependent backlash can be challenging, but by using θ_I and θ_L and the applied bidirectional motion a mea-

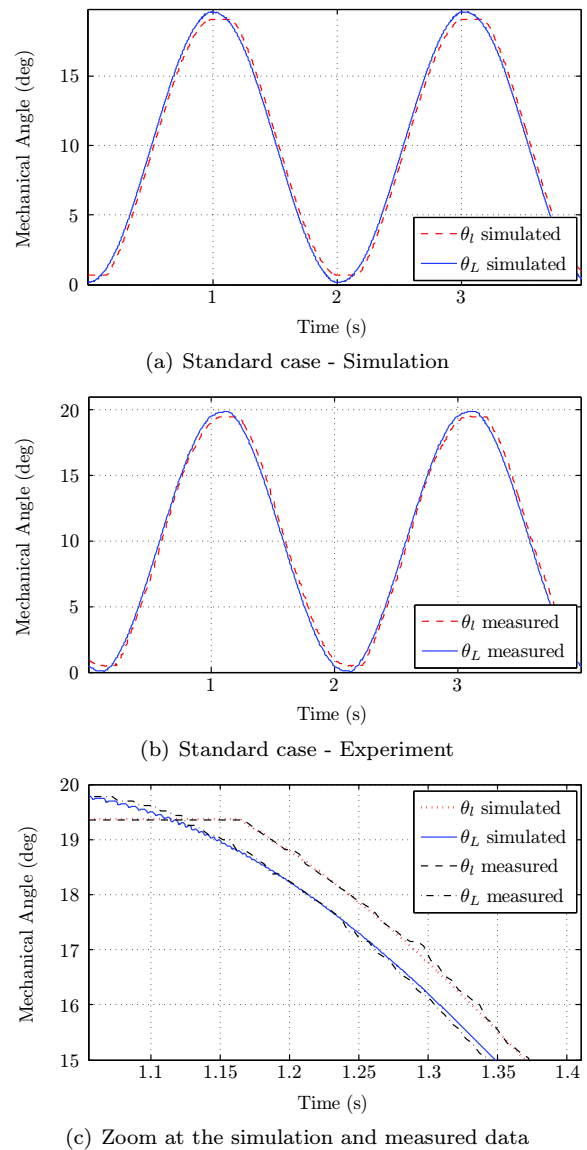


Fig. 9 Simulation and experimental results of the standard case.

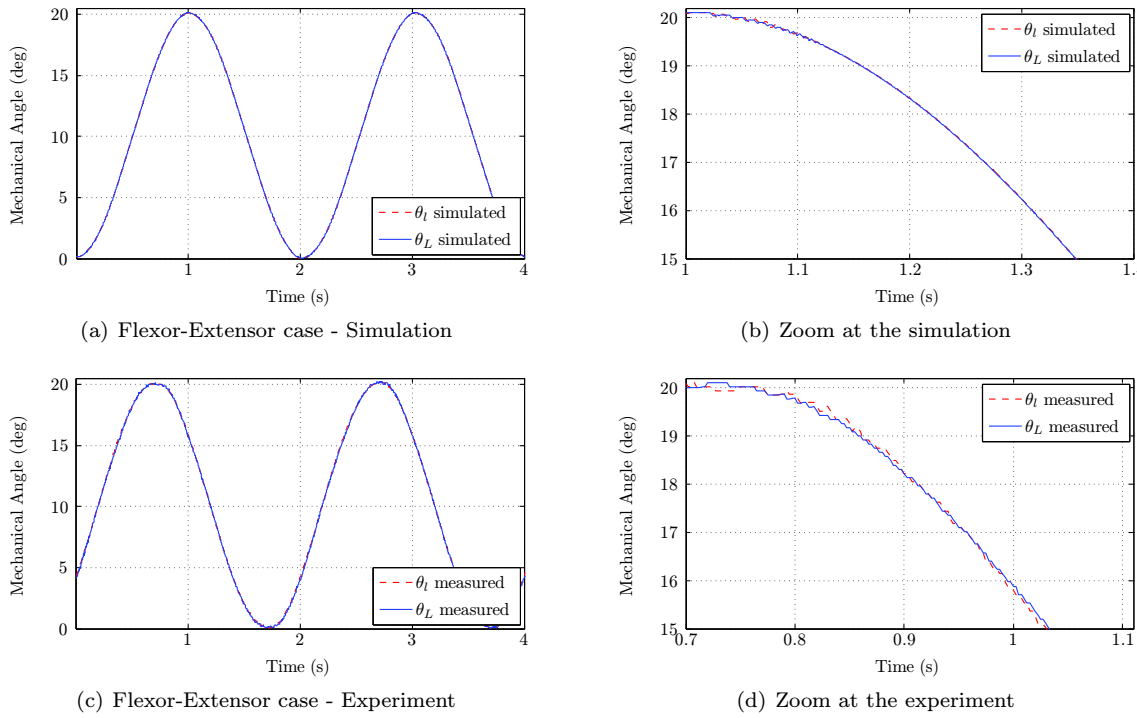


Fig. 10 Simulation and experimental results of the flexor-extensor case.

surement of the remaining level of the backlash could be approximated [35]. In order to have a quantitative comparison a specific mean value is defined as:

$$\beta_c = \frac{1}{T} \int_T |\theta_I(t) - \theta_L(t)| dt, \quad (25)$$

where T is the period of the sinusoid that was given as a velocity reference. This mean value gives a comparison basis to compare the results and gives an approximation of the remaining level of backlash. It averages the difference of the direct measure and the calculated position of the load through one period of the bidirectional motion.

Table 1 shows the quantitative results where the standard case almost exactly reproduced the original backlash value. In the standard case, the difference between the simulation and the experiment is about 1% (2.1×10^{-4} rad). This value for the proposed flexor-extensor case is slightly larger than 25% (-3.1×10^{-4} rad), which is caused presumably by the relatively low positional resolution, however the difference in absolute terms matches well with the preceding case. Comparing the standard and flexor-extensor case, simulation shows $1 - \frac{0.00087}{0.01913} = 95.45\%$ reduction in the average of the remaining backlash. Real measurement showed $1 - \frac{0.00118}{0.01892} = 93.76\%$ reduction that is just slightly less compared to the simulation result.

All constants that are used during the simulations are listed in Table 2.

Table 1 Comparison of test results

Configuration / Method	β_c
Standard / simulation	0.01913 rad
Standard / experiment	0.01892 rad
Flexor-Extensor / simulation	0.00087 rad
Flexor-Extensor / experiment	0.00118 rad

Table 2 List of constants

B_m	$8 \times 10^{-5} \frac{Nm \cdot s}{rad}$	J_m	$1.76 \times 10^{-7} kg \cdot m^2$
B_g	$1.1 \times 10^{-4} \frac{Nm \cdot s}{rad}$	J_g	$0.4 \times 10^{-7} kg \cdot m^2$
B_l	$1.05 \times 10^{-1} \frac{Nm \cdot s}{rad}$	J_l	$7.5 \times 10^{-4} kg \cdot m^2$
K	$1.46 \times 10^6 \frac{N}{m}$	b	$7.8 \times 10^{-4} m$
r_m, r_{g2}	$3.7 \times 10^{-3} m$	r_{g1}, r_l	$3.7 \times 10^{-2} m$

7 Conclusion

A new improved actuation system for robotic joints has been described in this paper. The proposed joint consists of two stepper motors that are operated in a flexor-extensor fashion inspired by the structure of human limbs. With this solution, a method was given for mini-

mizing the effect of backlash by applying a simple high-level control algorithm. Real measurement data show a good match with simulation results and clearly supports the practical applicability of the approach. Based on the experimental results the mean reduction of the backlash was over 90%.

Acknowledgments

The Office of Naval Research (ONR) that supports the multidisciplinary doctoral school at the Faculty of Information Technology of the Pázmány Péter Catholic University and the Bolyai János Research Scholarship of the Hungarian Academy of Sciences are gratefully acknowledged. The authors are also grateful to Ákos Tar and the members of the Robotics lab for the discussions and their suggestions. Special thanks go to Zsófia Cserey, and Miklós Gyöngy.

References

1. S. Villwock and M. Pacas, "Time-Domain identification method for detecting mechanical backlash in electrical drives," *Industrial Electronics, IEEE Transactions on*, vol. 56, no. 2, pp. 568–573, 2009.
2. M. Ruderman, F. Hoffmann, and T. Bertram, "Modeling and identification of elastic robot joints with hysteresis and backlash," *Industrial Electronics, IEEE Transactions on*, vol. 56, no. 10, pp. 3840–3847, 2009.
3. L. Marton and B. Lantos, "Modeling, identification, and compensation of Stick-Slip friction," *Industrial Electronics, IEEE Transactions on*, vol. 54, no. 1, pp. 511–521, 2007.
4. S. Villwock and M. Pacas, "Deterministic method for the identification of backlash in the time domain," in *Industrial Electronics, 2006 IEEE International Symposium on*, vol. 4, 2007, pp. 3056–3061.
5. R. Merzouki, J. Davila, L. Fridman, and J. Cadiou, "Backlash phenomenon observation and identification in electromechanical system," *Control Engineering Practice*, vol. 15, no. 4, pp. 447–457, 2007.
6. P. Rostalski, T. Besselmann, M. Baric, F. Van Belzen, and M. Morari, "A hybrid approach to modelling, control and state estimation of mechanical systems with backlash," *International Journal of Control*, vol. 80, no. 11, pp. 1729–1740, 2007.
7. S. Villwock and M. Pacas, "Application of the Welch-Method for the identification of two- and Three-Mass-Systems," *Industrial Electronics, IEEE Transactions on*, vol. 55, no. 1, pp. 457–466, 2008.
8. M. F. Lima, J. A. Machado, and M. Crisostomo, "Experimental backlash study in mechanical manipulators," *Robotica*, vol. 29, no. 02, pp. 211–219, 2011.
9. N. H. Kim, U. Y. Huh, and J. G. Kim, "Fuzzy position control of motor plant with backlash," in *Industrial Electronics Society, 2004. IECON 2004. 30th Annual Conference of IEEE*, vol. 3, 2005, pp. 3190–3195.
10. A. Lagerberg and B. Egardt, "Backlash estimation with application to automotive powertrains," *Control Systems Technology, IEEE Transactions on*, vol. 15, no. 3, pp. 483–493, 2007.
11. L. Marton and B. Lantos, "Control of mechanical systems with stibbeck friction and backlash," *Systems and Control Letters*, vol. 58, no. 2, pp. 141–147, 2009.
12. L. Marton, "Adaptive friction compensation in the presence of backlash," *Journal of Control Engineering and Applied Informatics*, vol. 11, no. 1, pp. 3–9, 2009.
13. M. Nordin and P. Gutman, "Controlling mechanical systems with backlash—a survey," *Automatica*, vol. 38, no. 10, pp. 1633–1649, 2002.
14. R. Kalantari and S. Foomanr, "Backlash nonlinearity modeling and adaptive controller design for an electromechanical power transmission system," *Scientia Iranica Transaction B: Mechanical Engineering*, vol. 16, no. 6, pp. 463–469, 2009.
15. R. Merzouki and J. Cadiou, "Estimation of backlash phenomenon in the electromechanical actuator," *Control Engineering Practice*, vol. 13, no. 8, pp. 973–983, 2005.
16. H. Mokhtari and F. Barati, "A new scheme for a mechanical load position control driven by a permanent magnet DC motor and a nonzero backlash gearbox," in *Industrial Electronics, 2006 IEEE International Symposium on*, vol. 3, 2007, pp. 2052–2057.
17. M. Gruzman, H. I. Weber, and L. L. Menegaldo, "Time domain simulation of a target tracking system with backlash compensation," *Mathematical Problems in Engineering*, pp. 1–27, 2010.
18. G. E. Hovland, S. Hanssen, E. Gallestey, S. Moberg, T. Brogardh, S. Gunnarsson, and M. Isaksson, "Nonlinear identification of backlash in robot transmissions," in *Proceedings of the 33rd ISR (International Symposium on Robotics)*, Stockholm, 2002, pp. 7–11.
19. B. J. Jung, J. S. Kong, B. H. Lee, S. M. Ahn, and J. G. Kim, "Backlash compensation for a humanoid robot using disturbance observer," in *Industrial Electronics Society, 2004. IECON 2004. 30th Annual Conference of IEEE*, vol. 3, 2005, pp. 2142–2147.
20. J. S. Kong, B. J. Jung, B. H. Lee, and J. G. Kim, "Nonlinear motor control using dual feedback controller," in *Industrial Electronics Society, 2005. IECON 2005. 31st Annual Conference of IEEE*, 2006, pp. 1–6.
21. A. Akhter and A. Shafie, "Advancement of android from ancient time to present time and contribution of various countries in the research and development of the humanoid platform," *International Journal of Robotics and Automation (IJRA)*, vol. 1, no. 2, pp. 42–56, 2010.
22. S. G. Robertz, L. Halt, S. Kelkar, K. Nilsson, A. Robertsson, D. Schar, and J. Sciffer, "Precise robot motions using dual motor control," in *Robotics and Automation (ICRA), 2010 IEEE International Conference on*, 2010, pp. 5613–5620.
23. R. Boudreau, X. Mao, and R. Podhorodeski, "Backlash elimination in parallel manipulators using actuation redundancy," *Robotica*, vol. 1, no. 1, pp. 1–10, 2010.
24. Y. Ohba, S. Katsura, and K. Ohishi, "Friction free bilateral robot based on twin drive control system considering two resonant frequencies," in *Industrial Electronics Society, 2005. IECON 2005. 31st Annual Conference of IEEE*, 2005, pp. 1–6.
25. C. Mitsantisuk, K. Ohishi, S. Urushihara, and S. Katsura, "Identification of twin direct-drive motor system with consideration of wire rope tension," in *Mechatronics, 2009. ICM 2009. IEEE International Conference on*, 2009, pp. 1–6.
26. R. Enoka, *Neuromechanics of Human Movement*, 4th ed. Human Kinetics, June 2008.
27. S. Lyshevski, "Electromechanical flight actuators for advanced flight vehicles," *Aerospace and Electronic Systems, IEEE Transactions on*, vol. 35, no. 2, pp. 511–518, 1999.
28. K. Tsui, N. Cheung, and K. Yuen, "Novel modeling and damping technique for hybrid stepper motor," *Industrial*

- Electronics, IEEE Transactions on*, vol. 56, no. 1, pp. 202–211, 2009.
29. P. Crnosija, B. Kuzmanovic, and S. Ajdukovic, “Microcomputer implementation of optimal algorithms for closed-loop control of hybrid stepper motor drives,” *Industrial Electronics, IEEE Transactions on*, vol. 47, no. 6, pp. 1319–1325, 2000.
 30. P. Krishnamurthy and F. Khorrami, “An analysis of the effects of Closed-Loop commutation delay on stepper motor control and application to parameter estimation,” *Control Systems Technology, IEEE Transactions on*, vol. 16, no. 1, pp. 70–77, 2008.
 31. A. I. Chirila, I. D. Deaconu, V. Navrapescu, M. Albu, and C. Ghita, “On the model of a hybrid step motor,” in *IEEE International Symposium on Industrial Electronics, 2008. ISIE 2008*, 2008, pp. 496–501.
 32. F. Belkhouche and S. Muzdeka, “A linearized model for permanent magnet stepper motors,” in *Industrial Electronics Society, 2003. IECON '03. The 29th Annual Conference of the IEEE*, vol. 1, 2003, pp. 301–305.
 33. T. Kenjo and A. Sugawara, *Stepping Motors and Their Microprocessor Controls*, 2nd ed. Oxford University Press, USA, Jan. 1994.
 34. F. Khorrami, P. Krishnamurthy, and H. Melkote, *Modeling and adaptive nonlinear control of electric motors*. Springer, 2003.
 35. A. Ming, M. Kajitani, C. Kanamori, and J. Ishikawa, “Measurement of transmission error including backlash in angle transmission mechanisms for mechatronic systems,” *JSME International Journal Series C Mechanical Systems, Machine Elements and Manufacturing*, vol. 44, no. 1, pp. 196–202, 2001.